



ChemSusChem

Chemistry–Sustainability–Energy–Materials

 **Chemistry
Europe**

European Chemical
Societies Publishing

Accepted Article

Title: Pulsed electrochemical carbon monoxide reduction on oxide-derived copper catalyst

Authors: Joshua M. Spurgeon, Jacob M. Strain, Saumya Gulati, and Sahar Pishgar

This manuscript has been accepted after peer review and appears as an Accepted Article online prior to editing, proofing, and formal publication of the final Version of Record (VoR). This work is currently citable by using the Digital Object Identifier (DOI) given below. The VoR will be published online in Early View as soon as possible and may be different to this Accepted Article as a result of editing. Readers should obtain the VoR from the journal website shown below when it is published to ensure accuracy of information. The authors are responsible for the content of this Accepted Article.

To be cited as: *ChemSusChem* 10.1002/cssc.202000464

Link to VoR: <https://doi.org/10.1002/cssc.202000464>

WILEY-VCH

Pulsed electrochemical carbon monoxide reduction on oxide-derived copper catalyst

Jacob M. Strain,^[a] Saumya Gulati,^[a] Sahar Pishgar,^[a] and Joshua M. Spurgeon*^[a]

[a] J. M. Strain, S. Gulati, S. Pishgar, Dr. J. M. Spurgeon
Conn Center for Renewable Energy Research
University of Louisville
216 Eastern Parkway, Louisville, KY, 40292 (USA)
*E-mail: joshua.spurgeon@louisville.edu

Supporting information for this article is given via a link at the end of the document

Abstract: Efficient electroreduction of carbon dioxide has been a widely pursued goal as a sustainable method to produce value-added chemicals while mitigating greenhouse gas emissions. Processes have been demonstrated for the electroreduction of CO₂ to CO at nearly 100% faradaic efficiency, and as a consequence, there has been growing interest in the further electroreduction of carbon monoxide. Oxide-derived copper catalysts have promising performance for the reduction of CO to hydrocarbons but have still been unable to achieve high selectivity to individual products. A pulsed-bias technique is one strategy for tuning electrochemical selectivity without changing the catalyst. Herein a pulsed-bias electroreduction of CO was investigated on oxide-derived copper catalyst. Increased selectivity for single-carbon products (i.e., formate and methane) was achieved for higher pulse frequencies (< 1 s pulse times), as well as an increase in the fraction of charge directed to CO reduction rather than hydrogen evolution.

Introduction

Developing viable routes to convert waste CO₂ to value-added chemicals is receiving increasing interest as a strategy to decrease greenhouse gas emissions.¹ Several techno-economic analyses have indicated that with sufficient performance improvements, several products could be commercially produced through electrochemical CO₂ reduction.^{2, 3} Copper is one of the few catalysts that has shown high activity for producing hydrocarbons and oxygenates through the carbon dioxide reduction reaction (CO₂RR).⁴ Oxide-derived copper (OD-Cu), wherein an oxidized Cu surface is subsequently electrochemically reduced, possesses a high electrochemically active surface area with a high density of grain boundaries, which has led to increased activity compared to planar Cu.^{5, 6} However, designing catalysts for very high CO₂RR selectivity to a single product is hindered by the scaling relations which limit the degree to which the binding energy can be simultaneously optimized for the various intermediate reactions in a multi-step reaction.⁷ For a simple single-carbon product like CO, several other catalysts have been

able to achieve near 100% faradaic efficiency (FE) from CO₂ at high current density.⁸

Thus, a promising approach to mitigate the limitations of the CO₂RR scaling relations is the further direct electrochemical reduction of CO in a second electrocatalytic system. Cascade electrolysis systems have been demonstrated by first reducing CO₂ to CO with Au or Ag, then subsequently flowing the CO to a second electrolyzer or catalyst for a more selective secondary reduction.^{9, 10} With OD-Cu, for instance, the grain boundary active sites promote adjacent CO binding and subsequent C-C bond formation, leading to higher FE for C₂ products like ethanol and acetate compared to conventional Cu for the electrochemical CO reduction reaction (CORR).¹¹ This approach has motivated significant recent study of CO reduction,^{12, 13} which has yielded advancements like > 90% FE for CORR at a partial current density of over 600 mA cm⁻², enabled by CO gas flow-through electrolyzer designs.¹⁴

Beyond modifications to the catalyst, the reaction branching pathway can also be tuned by affecting the dynamics at the electrochemical interface by pulsing the applied bias to the electrolyzer. This approach manipulates a complex interplay between the pulsing frequency and vertex potentials with the balance between reaction kinetics and mass transfer as well as the charging and discharging of the electrode double-layer capacitance.¹⁵ For potential pulses in the multi-second time range, improved CO₂ mass transport to the electrode during the rest pulse enabled modestly enhanced FE for CH₄ and C₂ products.¹⁶⁻¹⁸ In the sub-200 ms pulse time range, the charging/discharging of the electrode capacitance favored CO₂RR intermediate desorption and resulted in tunable and selective syngas (H₂+CO) formation.¹⁵ Pulsed-bias CO₂RR activity was also shown to depend strongly on the electrode geometric surface area, with the differences attributed to induction time and the rate of double-layer charging.¹⁹ Pulsed-bias electrolysis has further been demonstrated to have the added benefit of mitigating catalyst poisoning from contaminants or byproducts by repeated reduction/oxidation of the electrode interface to release or convert the undesired adsorbed species.^{20, 21} Despite the increasing

interest in electrochemical CO reduction, however, few if any reports exist on the ability of pulsed-bias conditions to direct the selectivity of CORR. Herein, we have investigated the effects of variable electrolysis parameters on the product distribution for reducing CO with a highly nanostructured OD-Cu catalyst surface.

Results and Discussion

First the behavior of OD-Cu for CORR under potentiostatic conditions without pulsed bias was established (see Experimental). After in situ reduction of the OD-Cu, current density vs. potential (J - E) behavior was measured to confirm the near absence of the peak corresponding to copper oxide reduction (Fig. S1). Fig. 1 shows the CORR product FEs and overall current density as determined at the end of a 60 min electrolysis. The results are the average of three redundant measurements at each potential. The product FE values (Table S1) are consistent with other reports for potentiostatic CORR on OD-Cu.^{12, 22} Minimum H₂ production was observed at -0.30 V vs. RHE, with a FE of 44.1%. Peak C₂₊ product formation occurred at -0.35 V vs. RHE, with FEs of 19.7% and 4.6% for ethanol and acetate, respectively, as well as trace propanol with a FE of 0.35%. At -0.40 V vs. RHE, the gaseous C₂ products ethylene and ethane were detected at a combined FE of 8.0%. At -0.25 and -0.30 V vs. RHE, the total FE to measured products was significantly below 100%, and we attribute the balance to continued restructuring and reduction of the electrode as well as unquantified acetaldehyde. Acetaldehyde, which is known to be an intermediate product on the way to ethanol formation,²² is highly volatile. Although the low concentration makes it difficult to quantify by GC with the dynamic flow mode used herein, a static-headspace method has permitted quantification by others.²² It was recently reported that acetaldehyde is a major product (~60% FE) at low overpotentials on nanoflower Cu,¹² making this a likely source for much of the missing charge in Fig. 1. Furthermore, a moderate drop in current density occurred during the 60 min electrolysis (Fig. S1), most likely due to a partial loss of the Cu wire mesh-like nanostructures over time as has been seen in other OD-Cu studies.^{5, 11}

A small amount of formate, HCOO⁻, (< 1.7% FE) is reported in Fig. 1 as an electrochemical CORR product on OD-Cu. The presence of formate as a product is noteworthy

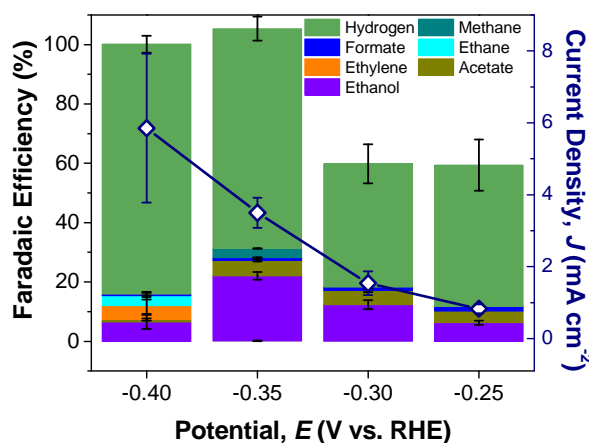


Fig. 1. Product distribution for CORR on OD-Cu in CO-saturated aqueous 0.1 M KOH. Overall current density (diamonds) is the value after 60 min. Values are the average of three measurements at each potential.

because other groups have reported that it may arise via a non-electrochemical route in CORR, perhaps as a hydration product.¹¹ Some formate is clearly generated through a non-electrochemical route, as it has been demonstrated to form under CORR conditions at open-circuit voltage (OCV) with a Cu electrode.¹² We performed additional control experiments to further elucidate the behavior of HCOO⁻ production on OD-Cu for CORR. Figure S2 shows the total formate production rate on OD-Cu at relevant potentials, including where no faradaic current passed, as well as the formate produced in the absence of an electrode. Only 0.09 μ mol of HCOO⁻ was detected without the OD-Cu catalyst, which increased to 0.95 μ mol for OD-Cu at 0 V vs. RHE and reached as high as 3.99 μ mol at -0.35 V vs. RHE.

While some formate is likely produced through a non-electrochemical CO hydration, this route alone cannot explain the observed potential-dependence of HCOO⁻ concentration. Instead, it is proposed that electrochemically generated OH⁻ from alkaline hydrogen evolution at higher localized concentration in the vicinity of surface-adsorbed CO on the electrode accelerates the rate of CO hydration to formate (see SI). Faradaic efficiency for formate by an indirect electrochemical route was therefore determined by subtracting the baseline molar production of HCOO⁻ in the 0.1 M KOH electrolyte with an OD-Cu electrode at open-circuit from the value measured at a given applied bias. Variation in the HCOO⁻ production under pulsed-bias conditions was even more pronounced, further indicating that a purely non-electrochemical route was not sufficient to explain the generation of formate. The formate production route, along with the proposed reaction pathways and cathodic half-reactions for the other products for alkaline CORR on OD-Cu are shown schematically in Figure 2.

For the pulsed-bias CORR experiments, the main parameter investigated for its effect on the product distribution was the pulse frequency. A square-wave pulse between a cathodic potential, E_c , at -0.35 V vs. RHE and a rest potential, E_r , at 0 V vs. RHE was used consistently throughout the study (Fig. 3a). The E_c value was selected as the potential for maximum CORR FE, including to C₂ products (Fig. 1). At the E_r potential, no steady-state faradaic current passes, which allows time for CO diffusion without promoting the local oxidation of the CORR products that might occur at more anodic potentials. Pulsed-bias CO measurements applied the potential square wave for 60 min, of which only half that time was spent at the active E_c reductive condition. After switching potentials, a transient current decayed over ~1 s before reaching a pseudo-steady-state current within the pulse. An example pulsed-bias current density vs. time profile is shown in Fig. 3b. Within each pulse, the current is a combination of non-faradaic capacitive charging current and the faradaic currents directing charge to CORR, the hydrogen evolution reaction (HER), and Cu reduction/oxidation. It is difficult to determine an unequivocal and quantifiable deconvolution of the faradaic and non-faradaic components of the charge passed. Although double-layer capacitive charging can be fit with an RC circuit exponential fit, the underlying baseline faradaic current is likely not constant and thus difficult to

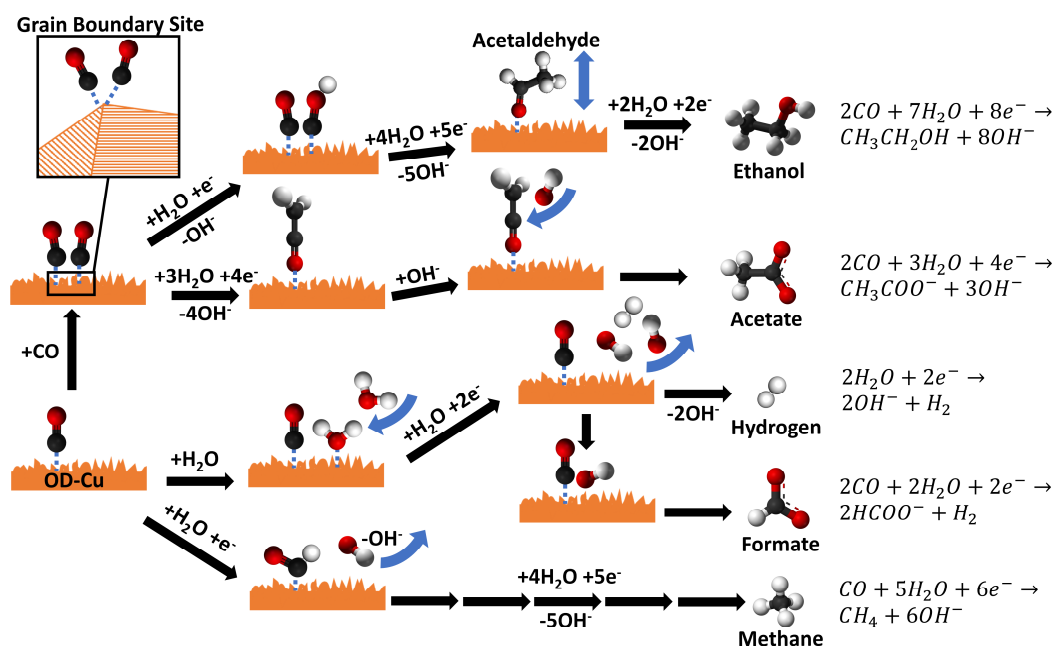


Fig. 2. Proposed reaction pathways for CORR on OD-Cu in 0.1 M KOH to the observed products. Cu grain boundaries promote adjacent CO binding and subsequent C-C bond formation. Acetaldehyde is a readily desorbed intermediate species on the reduction pathway to ethanol.²² Acetate formation is believed to proceed through hydroxide attack of a surface-bound ketene.¹¹

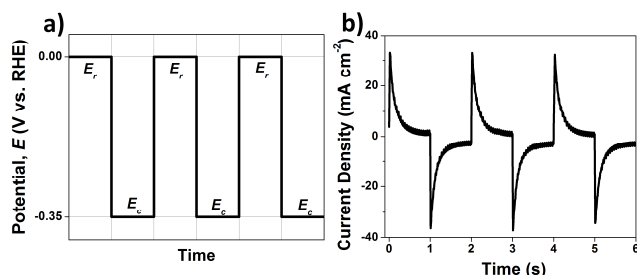


Fig. 3. (a) Pulsed-bias waveform alternating the OD-Cu potential between the cathodic potential, E_c , at -0.35 V vs. RHE and a rest potential, E_r , at 0 V vs. RHE. (b) Example pulsed-bias current density response for 1 s pulse times.

accurately quantify. Thus, rather than calculate FEs in pulsed-bias conditions, the selectivity in these experiments is reported as the product distribution by charge. Moreover, OD-Cu morphology after pulsing was investigated by SEM and capacitance measurements (Figs. S3-6, Table S2). With no clear trend in surface roughness observed with pulsing times, we attribute the variations in product distribution to the dynamic interfacial electrochemistry rather than changes in the catalyst.

Pulsing times varied from 10 ms to 50 s, covering the wide range of pulse frequencies reported in previous pulsed-bias studies on Cu for CO₂RR.¹⁵⁻²¹ Figure 4 shows the resulting product distributions measured at each pulse time along with the total measured charge required to produce all the detected products (Table S3). Each of the values are the average of three individual measurements. The total measured charge was determined by calculating the required charge to produce all the measured products from CO and H₂O reactants.

With increasingly longer pulses, the product distribution would be predicted to asymptote towards the values observed for non-pulsed continuous electrolysis as steady-state conditions increasingly dominate each pulse.¹⁵ However, the observed CORR products for 50 s pulse

times deviated appreciably from the values measured for continuous electrolysis (Fig. 4a). In particular, a lower fraction of ethanol and acetate was observed for long pulse times relative to the no-pulse condition. A control experiment was therefore conducted with a 30 min continuous electrolysis followed by 30 min at OCV with continued CO bubbling (i.e., a 1800 s pulse). The 1800 s pulse product distribution was consistent with the values measured for 50 s pulse times and also had notably lower fractions of ethanol and acetate compared to the no-pulse condition. We therefore attribute the reduced measured fraction of these liquid C₂ products to changes occurring during the rest periods of the pulsed electrolysis. Gaseous CH₄ and H₂ products, however, were observed in similar amounts. The discrepancy between the observed liquid products for long pulses and non-pulsed electrolysis is likely attributable to the volatility of ethanol and acetate, leading to the gradual vaporization of these products into the output CO stream at concentrations below the GC detection limit in the continuous dynamic flow mode used herein. Because the NMR liquid product quantification measures the accumulated product at the end of the experiment, the time spent under active CO bubbling at the rest potential for pulsed-bias conditions reduces the observed fraction of volatile liquid products relative to a continuous electrolysis. The reported product distribution by charge for ethanol and acetate under pulsed-bias is therefore a lower limit, and the actual fraction of C₂ species produced is assumed to be higher. However, precisely accounting for the volatile product with a static-headspace method is challenging for CORR due to the low solubility of CO, which makes steady-state reduction difficult in the absence of active CO bubbling.

For non-pulsed CORR electrolysis at -0.35 V vs. RHE, the faradaic efficiency for H₂ was 68.2%, and the total FE

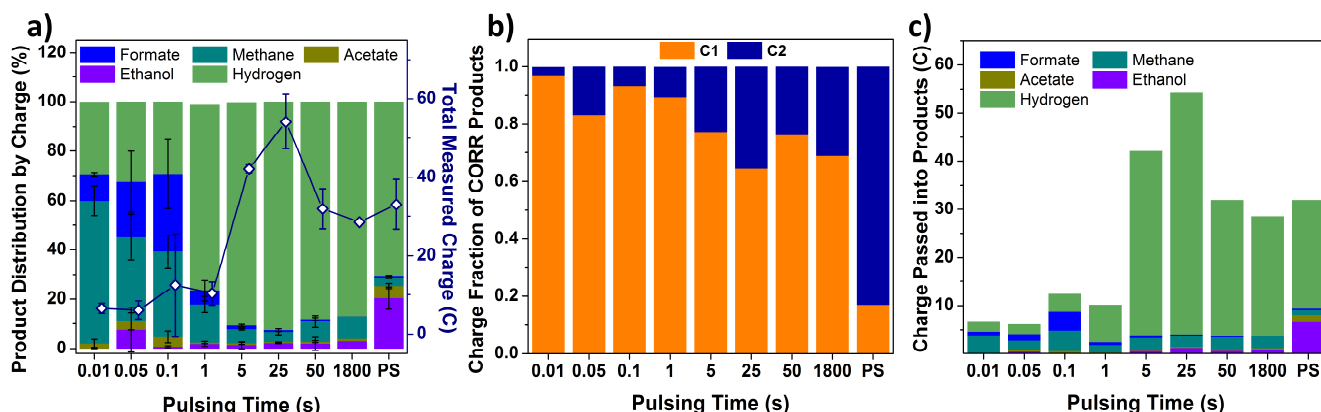


Fig. 4. (a) Product distribution vs. pulsing time along with the corresponding total measured charge (white diamonds, right axis) attributed to the detected products, and (b) the fraction of CORR products which are either one- or two-carbon species. (c) The total charge attributable to each detected product. The "PS" condition refers to a potentiostatic measurement at -0.35 V vs. RHE for 60 min.

for CORR was 28.8% (Fig. 1, Table S1). Accounting for faradaic current to undetected products, this is equivalent to a product distribution by charge of 70.3% for HER and 29.7% for CORR (Fig. 4a, Table S2). Vaporization of volatile liquid products during the rest period accounted for a decrease in the charge fraction of CORR, with a product distribution by charge for CORR of 13% for the 1800 s pulse time, and corresponding increase in HER to 87%. The HER charge fraction increased to as high as 92.4% at 25 s pulses, then decreased with decreasing pulse times to 29.3% for 10 ms pulses (Fig. 4a, Table S2). CORR became the dominant reaction over HER at 100 ms and shorter pulses, accounting for $\sim 70\%$ of the charge, although the total charge was lower in this pulse frequency range. While the partial charge for CORR products increased from 4.1 C at 25 s pulses to as high as 8.8 C at 100 ms pulses, the partial charge for HER decreased from 50.1 C to 3.6 C between the same conditions, respectively (Fig. 4c). Thus, the decrease in the total measured charge at shorter pulses can primarily be attributed to a decrease in the rate of HER. Interestingly, this finding is the reverse trend of the results observed in our previous pulsed-bias work on CO_2RR on Cu in neutral aqueous KHCO_3 , in which the rate of H_2 formation increased with shorter millisecond pulses.¹⁵ In that work, an increase in HER relative to CO_2RR at short pulse times was attributed to the constantly changing electric field due to double layer charging/discharging leading to desorption of the CO_2 reduction intermediates and subsequent promotion of HER. In the present case, CO binding and reduction is instead competing with alkaline HER, in which water-splitting occurs through a OH^- intermediate rather than a H^+ . We thus speculate that the non-faradaic current from charging/discharging which dominates short pulses in the ms regime could have a different effect on the binding energy and species adsorption which acts to inhibit HER in this situation. In addition, a less reductive potential (-0.35 V vs. RHE) was used for CORR in the present work compared to the potential (-1.0 V vs. RHE) applied for CO_2RR in the previous study, leaving less driving force for HER to overcome competing effects in the present study.¹⁵

Besides changing the relative rates of HER to CORR, pulsing frequency also had an effect on the charge distribution of carbonaceous products. For pulsed-bias electrolysis, a general trend was observed in which shorter pulses corresponded to a lower charge fraction of the CORR products being directed towards C_2 species (Fig. 4b). Only minor variation was observed in the CORR product distribution for pulse times > 5 s, which can be attributed to the majority of the active E_c period being in pseudo-steady-state for pulses of this duration. For pulses ≤ 1 s, however, more significant variation in the CORR product distribution occurred (Fig. 4a). The charge fraction of C_2 products was notably lower in the sub-second pulse range, reaching as low as 3.0% of the CORR products for 10 ms pulse times (Fig. 4b). While some pulsed-bias CO_2RR studies have reported notable enhancements in selectivity toward C_2 products at pulses in the 1 – 5 s range,^{16–18} pulsing at 100 ms and below decreased C_2 product formation.¹⁵ The short pulse time CORR results herein are consistent with previous reports in which the non-faradaic component is dominant at sub-second pulse times and the continuously changing interfacial energetics affect species adsorption and prevent the pseudo-steady-state needed to promote adjacent adsorbed CO^* species capable of C-C bond formation to C_2 products.

Furthermore, with the decreased HER and C_2 production at sub-second pulse times, the production of C_1 methane and formate species increased as a result. The partial charge for C_1 products varied from 2.6 C (0.4 C to formate, 2.2 C to methane) at 25 s pulses to 8.2 C (3.9 C to formate, 4.3 C to methane) at 0.1 s pulses (Fig. 4c, Fig. S7). If the strong component of non-faradaic current throughout the short pulse times inhibits HER and C-C bond formation, reduction of the single adsorbed CO becomes the preferred route. Full reduction and protonation of the CO leads to CH_4 .²³ As mentioned above, some formate is produced through a non-electrochemical hydration step, but the potential dependence of the formate concentration indicates an electrochemical pathway exists as well (Fig. S2). Increased formate production at short pulses is consistent with the favored reduction of a single adsorbed CO, as near-surface OH^- reacts with the CO to

make formate (see SI). At longer active cathodic pulse times, these reaction rates compete with diffusion of CO from the bulk to the electrode, permitting greater HER relative to CORR.

Conclusions

Herein, a pulsed-bias technique on a nanostructured Cu surface was investigated using the pulse time as a parameter for affecting the CORR selectivity. The 50% duty cycle used for pulsed-bias conditions resulted in appreciable loss of the volatile C₂ liquid products to the gas phase relative to a continuous process. Using pulses from 0.01 – 50 s, the selectivity to CORR was significantly enhanced at sub-second pulse times mainly due to a decrease in the rate of the competing HER, which is a different behavior than previously observed for CO₂ reduction in neutral electrolyte. Additionally, the shorter pulses greatly enhanced the direction of charge to C₁ relative to C₂ products, reaching a ratio as high as 97:3 at 10 ms pulse times. Consequently, sub-second pulse conditions had significantly higher fractions of the total charge resulting in the production of methane and formate. Further study with variable duty cycle and applied potential E_c during the cathodic pulse may yield additional conditions for controlling the selectivity of CORR on Cu. Pulsed-bias studies such as these are a promising way to achieve an additional systems-level control over the electroreduction reaction as a way to complement the design of catalyst materials for high selectivity.

Experimental Section

Membranes and Chemicals

All reagents were used as received, except for KOH (reagent grade, Amresco) which was purified using the K form of Chelex 100 (received as the Na form, Sigma-Aldrich). All electrolyte solutions were prepared in 18 M Ω -cm water. The anion exchange membrane used in the electrochemical cell was 100 μ m thick Selemion (AGC Engineering Co., Ltd.), pretreated by soaking in a bath of 1 M KOH for over 24 hours to ensure there were negligible membrane contaminants in the electrolyte.²⁴

Electrode Fabrication

Oxide-derived copper (OD-Cu) electrodes were prepared from Cu foil (0.127 mm thick, 99.9%, Alfa Aesar) following a published method.^{5,11} The Cu foil was sonicated for 30 min in acetone and isopropanol for cleaning and then electropolished in 85% phosphoric acid (Macron Fine Chemicals) at 2.0 V vs. a secondary Cu foil for 5 min under vigorous stirring. Both sides of the foil were electropolished. The foil was then rinsed in 18 M Ω -cm water and dried under nitrogen. The Cu foil was subsequently placed in a muffle furnace under ambient air for thermal oxidation with a 1.5 h ramp up to 500 °C, 12 h at

500 °C, and then a 10 h ramp down to room temperature. The CuO_x foil was then placed in the electrochemical cell with ~ 3 cm² exposed to the 0.1 M KOH electrolyte and reduced at -0.5 V vs. RHE for 45 - 60 min until the current density reached a steady-state value for 5 min at \leq 5 mA cm⁻². Previous XPS and XRD characterization has demonstrated a surface of Cu(II) present as Cu₂O after thermal oxidation, converting to primarily Cu(0) after the electrochemical reduction step, with the return of a thin oxide layer and Cu(II) and Cu(I) due to residual anodic surface oxidation during pulsed-bias operation.^{5, 15}

Electrochemical Measurements

Electrochemical CO reduction experiments were performed with a BioLogic SP-200 potentiostat. The electrochemical cell was made of polycarbonate plates and set up for a three-electrode experiment with the OD-Cu foil as the working electrode, Pt mesh as the counter electrode separated from the cathode compartment by the membrane, and a Ag/AgCl (CH Instruments, Inc.) in 3.0 M KCl as the reference electrode.¹⁵ Potentials were calculated from the equation $V_{RHE} = V_{Ag/AgCl} + 0.210 + 0.059 \cdot \text{pH}$. The pH of the 0.1 M KOH electrolyte was 13. Following electrochemical reduction of the OD-Cu, the catholyte was flushed and replaced with fresh 0.1 M KOH with a catholyte volume of 7.5 mL. Prior to CORR measurements, the electrolyte in both the cathode and anode chambers was bubbled with CO (99.99%, Specialty Gases) at 10 sccm for 20 min and potentiostatic electrochemical impedance spectroscopy (PEIS) was then used to measure the uncompensated cell resistance. Typical resistances for the cell ranged from 15 – 28 Ω . The potentiostat was then set to compensate for 85% of the uncompensated resistance during the electrochemical CORR experiment, which was conducted with a steady CO flow rate of 10 sccm through a bubbler with 4 - 5 μ m pores in the catholyte at the base of the OD-Cu electrode. Electrochemical surface area (ECSA) measurements were performed to obtain the double-layer capacitance values of the OD-Cu electrodes before and after pulsed-bias electrolysis.²⁵ A cyclic voltammogram was produced at potentials without faradaic current (0.02 to 0.26 V vs. RHE) and the non-faradaic current was plotted versus the scan rate to calculate the double-layer capacitance. The scan rates were 10, 20, 40, 60, and 80 mV s⁻¹. The roughness factor was estimated by dividing the calculated OD-Cu electrode capacitance by the approximate capacitance of atomically smooth Cu (29 μ F).⁶

Product Analysis

CO reduction products were measured by gas chromatography (GC, SRI 8610) and nuclear magnetic resonance (NMR) spectroscopy for the gas and liquid products, respectively. Both instruments were calibrated with standard gases or liquid solutions. The concentration of gaseous products was measured at 15, 30, 45, and 60 min. The liquid products were collected at 0 min and 60 min for each electrolysis experiment. The moles of each

liquid product were determined by taking the difference between the final and initial concentrations. A 400 μL aliquot of the catholyte was mixed with 100 μL of D_2O that contained ~ 100 ppm dimethyl sulfoxide (DMSO, ACS grade, Amresco). The peak area of the DMSO internal standard was compared to the peak area of each liquid product in $^1\text{H-NMR}$ using a Varian 700 MHz cold-probe while using a water peak suppression technique. For non-pulsed experiments, the faradaic efficiency was determined directly by comparing the charge required to produce the measured products to the total charge passed as measured by the potentiostat. Because of the constantly shifting convolution of faradaic and transient non-faradaic (i.e., double-layer capacitive charging) currents during pulsed-bias conditions, it is not straightforward to calculate faradaic efficiency for pulsed-bias experiments. Instead, for pulsed-bias experiments the selectivity was based on the product distribution by charge, which was calculated by comparing the charge required to produce a given product relative to the charge required to produce all the measured products. Thus, the product distribution by charge is the same as faradaic efficiency except that it does not account for charge passed which did not result in a detected product.

Catalyst Characterization

A scanning electron microscope (FEI NOVA nano-SEM 600) was used to image the surface morphology of the Cu foil. A Bruker D8 powder X-ray diffraction (XRD) system was used for crystal structure and phase analysis using non-monochromated Cu-K α radiation produced by an X-ray tube operated at 40 kV and 40 mA. The sample XRD patterns were scanned between 30-80° at a scan speed of 4 s per step with a step size of 0.02°.

Acknowledgements

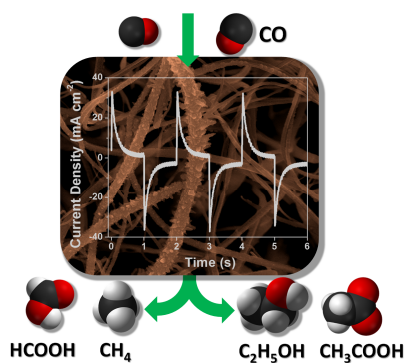
The authors acknowledge support from the Conn Center for Renewable Energy Research at the University of Louisville.

Keywords: carbon monoxide • reduction • pulsed bias • catalysis • electrochemistry

Notes and references

- [1] O. Bushuyev, P. De Luna, C. T. Dinh, L. Tao, G. Saur, J. van de Lagemaat, S. O. Kelly and E. H. Sargent, *Joule*, **2018**, 2, 825-832.
- [2] J. M. Spurgeon and B. Kumar, *Energy Environ. Sci.*, **2018**, 11, 1536-1551.
- [3] M. Jouny, W. Luc and F. Jiao, *Ind. Eng. Chem. Res.*, **2018**, 57, 2165-2177.
- [4] K. P. Kuhl, E. R. Cave, D. N. Abram and T. F. Jaramillo, *Energy Environ. Sci.*, **2012**, 5, 7050-7059.
- [5] C. W. Li and M. W. Kanan, *J. Am. Chem. Soc.*, **2012**, 134, 7231-7234.
- [6] Y. W. Lum, B. B. Yue, P. Lobaccaro, A. T. Bell and J. W. Ager, *J. Phys. Chem. C*, **2017**, 121, 14191-14203.
- [7] J. Perez-Ramirez and N. Lopez, *Nature Catalysis*, **2019**, 2, 971-976.
- [8] B. A. Rosen, A. Salehi-Khojin, M. R. Thorson, W. Zhu, D. T. Whipple, P. J. A. Kenis and R. I. Masel, *Science*, **2011**, 334, 643-644.
- [9] N. Theaker, J. Strain, B. Kumar, J. P. Brian, S. Kumari and J. M. Spurgeon, *Electrochim. Acta*, **2018**, 274, 1-8.
- [10] Gurudayal, D. Perone, S. Malani, Y. Lum, S. Haussener and J. W. Ager, *ACS Appl. Energy Mater.*, **2019**, 2, 4551-4559.
- [11] C. W. Li, J. Ciston and M. W. Kanan, *Nature*, **2014**, 508, 504-507.
- [12] L. Wang, S. Nitopi, A. B. Wong, J. L. Snider, A. C. Nielander, C. G. Morales-Guio, M. Orazov, D. C. Higgins, C. Hahn and T. F. Jaramillo, *Nature Catalysis*, **2019**, 2, 702-708.
- [13] H. Zhang, J. Li, M.-J. Cheng and Q. Lu, *ACS Catal.*, **2019**, 9, 49-65.
- [14] M. Jouny, W. Luc and F. Jiao, *Nature Catalysis*, **2018**, 1, 748-755.
- [15] B. Kumar, J. P. Brian, V. Atla, S. Kumari, K. A. Bertram, R. T. White and J. M. Spurgeon, *ACS Catal.*, **2016**, 6, 4739-4745.
- [16] J. Yano, T. Morita, K. Shimano, Y. Nagami and S. Yamasaki, *J. Solid State Electrochem.*, **2007**, 11, 554-557.
- [17] J. Yano and S. Yamasaki, *J. Appl. Electrochem.*, **2008**, 38, 1721-1726.
- [18] S. Ishimaru, R. Shiratsuchi and G. Nogami, *J. Electrochem. Soc.*, **2000**, 147, 1864-1867.
- [19] K. W. Kimura, K. E. Fritz, J. Kim, J. Suntivich, H. D. Abruna and T. Hanrath, *Chemsuschem*, **2018**, 11, 1781-1786.
- [20] G. Nogami, H. Itagaki and R. Shiratsuchi, *J. Electrochem. Soc.*, **1994**, 141, 1138-1142.
- [21] A. Engelbrecht, C. Uhlig, O. Stark, M. Hammerle, G. Schmid, E. Magori, K. Wiesner-Fleischer, M. Fleischer and R. Moos, *J. Electrochem. Soc.*, **2018**, 165, J3059-J3068.
- [22] E. Bertheussen, A. Verdager-Casadevall, D. Ravasio, J. H. Montoya, D. B. Trimarco, C. Roy, S. Meier, J. Wendland, J. K. Norskov, I. E. L. Stephens and I. Chorkendorff, *Angew. Chem.-Int. Edit.*, **2016**, 55, 1450-1454.
- [23] A. A. Peterson and J. K. Norskov, *J. Phys. Chem. Lett.* **2012**, 3, 2, 251-258.
- [24] J. M. Strain and J. M. Spurgeon, *Journal of Co2 Utilization*, **2020**, 35, 298-302.
- [25] C. C. L. McCrory, S. Jung, I. M. Ferrer, S. M. Chatman, J. C. Peters and T. F. Jaramillo, *J. Am. Chem. Soc.*, **2015**, 137, 4347-4357.

Entry for the Table of Contents



Variable pulsing frequency in a pulsed-bias electrochemical CO reduction affected selectivity and favored methane and formate at short pulse times. Pulsed-bias electrosynthesis enables some control of product selectivity that can be complementary to catalyst design. This type of CO reduction can be coupled to high efficiency reduction of CO₂ to CO for a two-step electrosynthesis of useful products from CO₂.